

The Herschel Dwarf Galaxy Survey
I. Properties of the low-metallicity ISM from
PACS spectroscopy
(D. Cormier et al. 2015, A&A, 578, 53)

Reporter: Y. Tamura (IoA, UTokyo)
Journal club @ IoA
20-Nov-2015

Abstract

低金属環境下での FIR fine structure line の“出方”が違うが、なぜかはよくわかっていない。

目的は、低金属 ISM をもつ dwarf での FIR line の出方をしらべ、説明すること。

- PACS による 48 dwarfs の FIR line 観測
- line/TIR ratio と各種物理量の相関関係
- Cloudy 輻射輸送モデル

Context. The far-infrared (FIR) lines are important tracers of the cooling and physical conditions of the interstellar medium (ISM) and are rapidly becoming workhorse diagnostics for galaxies throughout the universe. There are clear indications of a different behavior of these lines at low metallicity that needs to be explored.

Aims. Our goal is to explain the main differences and trends observed in the FIR line emission of dwarf galaxies compared to more metal-rich galaxies, and how this translates in ISM properties.

Methods. We present *Herschel*/PACS spectroscopic observations of the [C II] 157 μm , [O I] 63 and 145 μm , [O III] 88 μm , [N II] 122 and 205 μm , and [N III] 57 μm fine-structure cooling lines in a sample of 48 low-metallicity star-forming galaxies of the guaranteed time key program Dwarf Galaxy Survey. We correlate PACS line ratios and line-to- L_{TIR} ratios with L_{TIR} , $L_{\text{TIR}}/L_{\text{B}}$, metallicity, and FIR color, and interpret the observed trends in terms of ISM conditions and phase filling factors with Cloudy radiative transfer models.

Results. We find that the FIR lines together account for up to 3 percent of L_{TIR} and that star-forming regions dominate the overall emission in dwarf galaxies. Compared to metal-rich galaxies, the ratios of [O III]₈₈/[N II]₁₂₂ and [N III]₅₇/[N II]₁₂₂ are high, indicative of hard radiation fields. In the photodissociation region (PDR), the [C II]₁₅₇/[O I]₆₃ ratio is slightly higher than in metal-rich galaxies, with a small increase with metallicity, and the [O I]₁₄₅/[O I]₆₃ ratio is generally lower than 0.1, demonstrating that optical depth effects should be small on the scales probed. The [O III]₈₈/[O I]₆₃ ratio can be used as an indicator of the ionized gas/PDR filling factor, and is found to be ~ 4 times higher in the dwarfs than in metal-rich galaxies. The high [C II]/ L_{TIR} , [O I]/ L_{TIR} , and [O III]/ L_{TIR} ratios, which decrease with increasing L_{TIR} and $L_{\text{TIR}}/L_{\text{B}}$, are interpreted as a combination of moderate far-UV fields and a low PDR covering factor. Harboring compact phases of a low filling factor and a large volume filling factor of diffuse gas, the ISM of low-metallicity dwarf galaxies has a more porous structure than that of metal-rich galaxies.

Key words. galaxies: dwarf – infrared: ISM – photon-dominated region (PDR) – techniques: spectroscopic – radiative transfer – HII regions

- 電離ガス/PDRの filling factor は、通常より高い
- line-to-TIR ratio が高いのは、moderate FUV 輻射場と low PDR filling factor のせい。すかすかな構造

- Dwarf では FIR line coolant の寄与が通常(Z-rich galaxies)より大きく (TIR の 3% まで)
- 星形成領域が全 luminosity を dominate
- 輻射場は硬い

1. Introduction

- ❖ Low-metallicity environments are good for examining conditions for SF at high- z .
 - ❖ How do the physical conditions of SF regions vary as function of metallicity?
 - ❖ What controls the energy balance (h/c) in different ISM phases / morphology?
 - ❖ What are the roles of the different ISM phases in integrated view of galaxies?
- ❖ FIR line spectroscopy is important for ISM physics (FUV flux, n_H , T , filling factor).
 - ❖ [CII]157, [OI]63,145 are important coolants ($n_H > 10$ /cc, $T \sim 100$ -300 K).
 - ❖ [NII]122,205 and [OIII]52,88 are tracers of ionized gas.
- ❖ [CII] brightest cooling line in SF galaxies (0.1-1% of L_{fir}). But, additional lines are required to characterize ISM conditions.
- ❖ FIR lines in dwarfs are *exceptionally bright* compared to dust/CO emission.
 - ❖ While CO is photo-dissociated, H₂ can survive owing to self-shielding.
 - ❖ Such “CO-dark gas” is seen in C+. --> FIR lines as calibrators at high- z .
- ❖ Herschel “Dwarf Galaxy Survey (DGS)” (Madden+13)
 - ❖ PACS/SPIRE spectroscopy for 50 dwarfs with $\sim 1/40$ -1 Z_{sun} , SFR $\sim 5e-4$ - 25 Mo/yr, irregulars-spirals, $D < 200$ Mpc.
 - ❖ (Remy-Ruyer+13 for photometry, revealing warmer dust than metal-rich galaxies, excess emission in submm, lower $M_{\text{dust}}/M_{\text{gas}}$ ratio.)
- ❖ Focusing on PACS results for 48 dwarfs in this paper.

2. Data

§2.1. Herschel PACS spectroscopy

- ❖ PACS spectrometer (Poglitsch+10)
- ❖ 5x5 spatial pixels ("spaxels") covering 47" x 47"
- ❖ $\lambda = 60\text{-}160\ \mu\text{m} \Rightarrow$ beam size: 9" - 12", resolution: 90 - 240 km/s

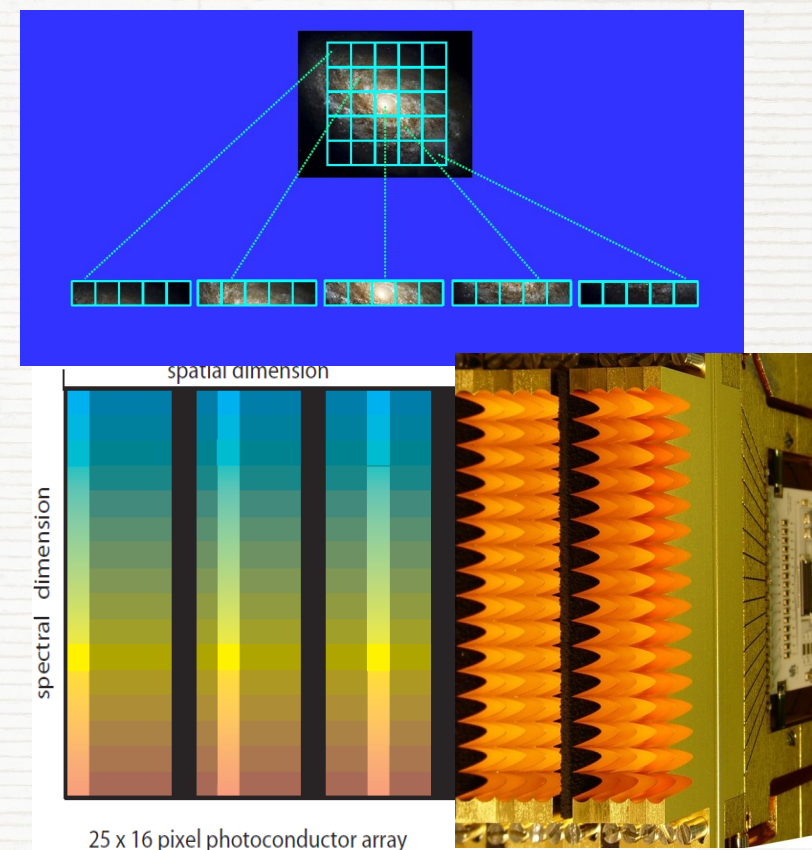


Zermatt - 20 Sep 2010

Instrument Concept - Spectrometer

Integral field spectroscopy

- range 55 - 210 μm
- IFU: 5 x 5 spaxels, image slicer
- Each spaxel 9.4" x 9.4"
- long-slit grating spectrograph (R \sim 1500)
- Two 16 x 25 Ge:Ga photoconductor arrays (stressed/unstressed)
- point source detection limit $3 \dots 20 \times 10^{-18}\ \text{W/m}^2$ (5σ , 1h)



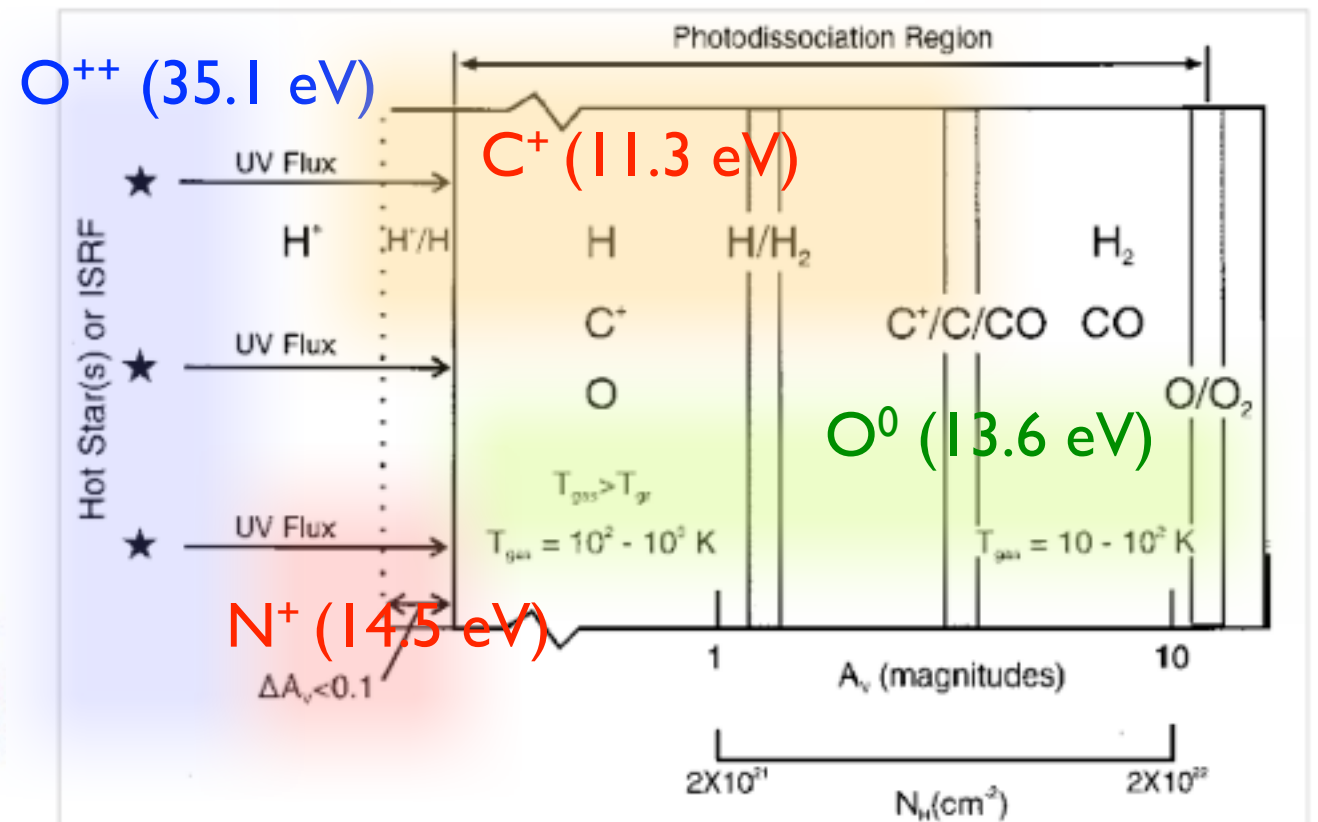
2. Data

§2.1.2. properties of FIR lines

Table 1. Characteristics of the PACS FIR fine-structure cooling lines.

Species	λ [μm]	Transition	IP [eV]	$\Delta E/k^a$ [K]	n_{crit} [cm^{-3}]
[C II]	157.7	$^2\text{P}_{3/2}-^2\text{P}_{1/2}$	11.3	91	$50^b, 2.8 \times 10^3$
[N II]	121.9	$^3\text{P}_2-^3\text{P}_1$	14.5	188	310
[N II]	205.2	$^3\text{P}_1-^3\text{P}_0$	14.5	70	48
[N III]	57.3	$^3\text{P}_{3/2}-^3\text{P}_{1/2}$	29.6	251	3.0×10^3
[O I]	63.2	$^3\text{P}_1-^3\text{P}_2$	-	228	4.7×10^5
[O I]	145.5	$^3\text{P}_0-^3\text{P}_1$	-	327	9.5×10^4
[O III]	88.4	$^3\text{P}_1-^3\text{P}_0$	35.1	163	510

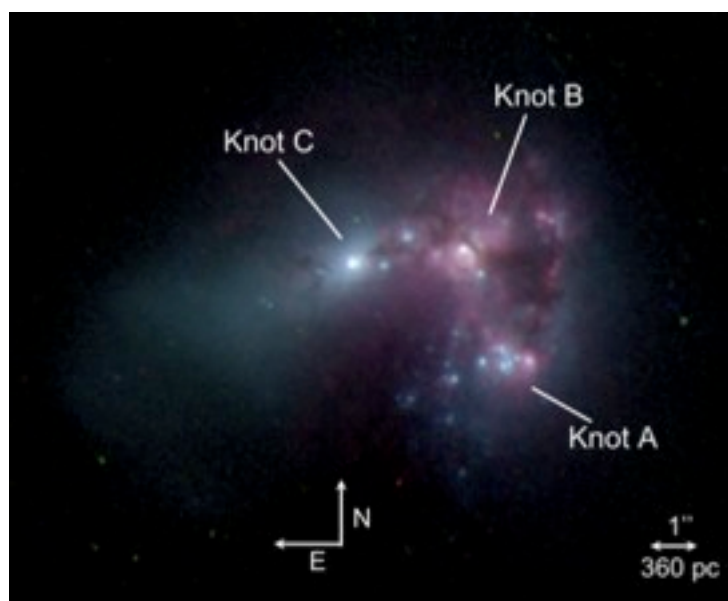
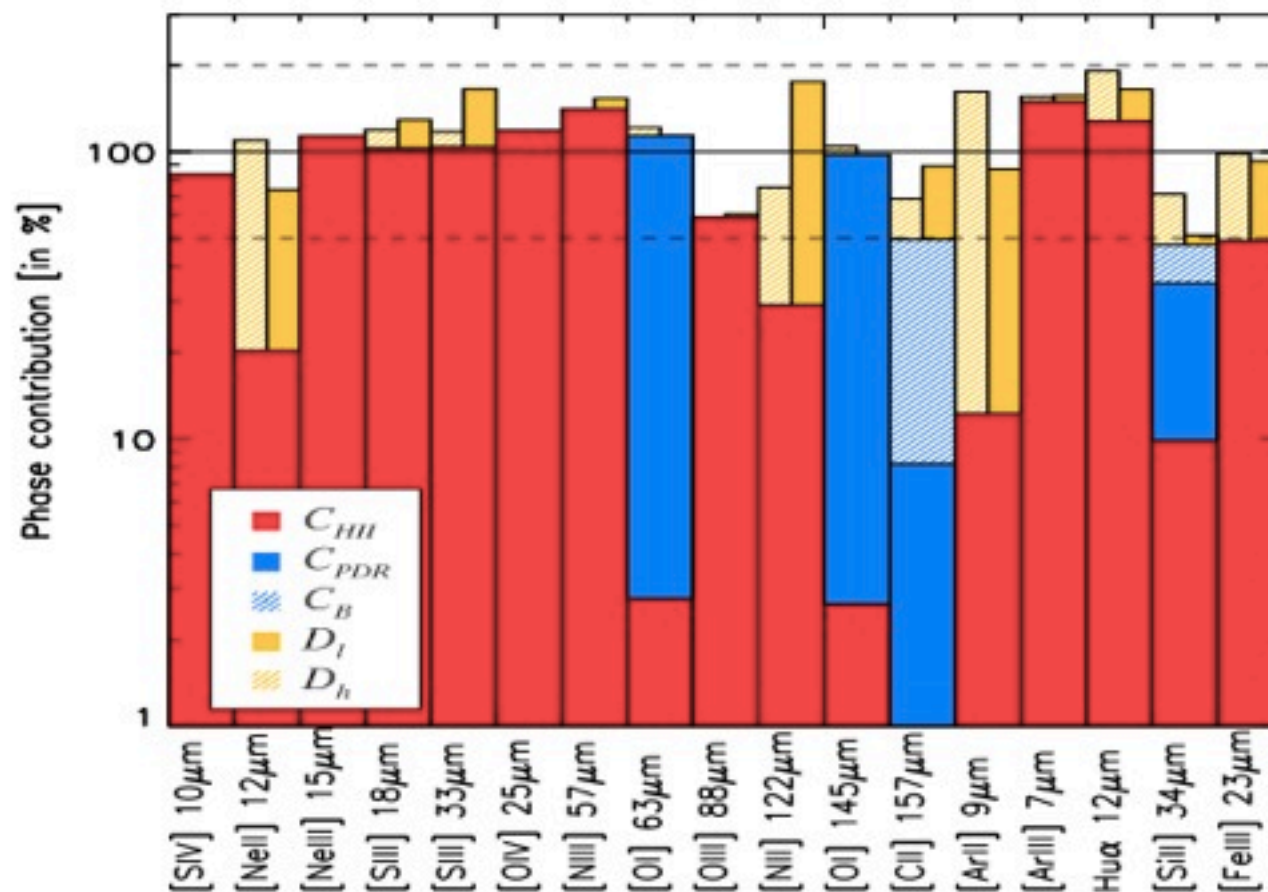
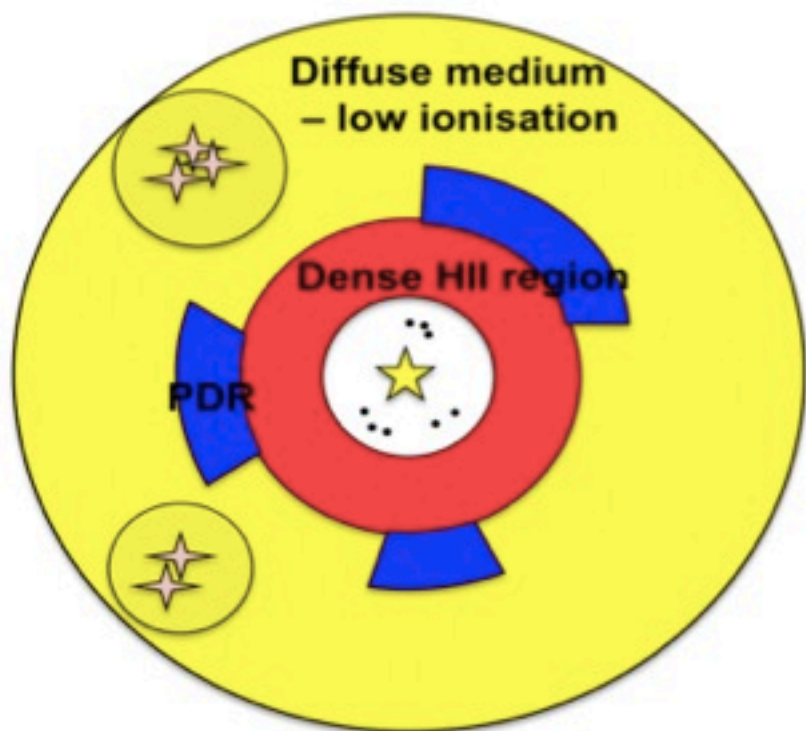
Notes. Values taken from [Madden et al. \(2013\)](#). The IP for [O II] is 13.62 eV. ^(a) Excitation temperature $\Delta E/k$ required to populate the transition level from the ground state. ^(b) Critical density for collisions with electrons.



Tielens & Hollenbach 2005, Phys. Rev.

- ❖ [CII]157: carbon is 4th abundant element. coming from both ionized and PDR gas.
- ❖ [NII]122, 205: (diffuse) ionized gas. 122/205 ratio is n_e tracer.
- ❖ [NIII]57: ionized gas (HII reg). [NIII]/[NII] as T_{eff} tracer
- ❖ [OI]63, 145: warm, dense neutral gas. can be affected by optical depth effect (self-absorption)
- ❖ [OIII]88: HII regions, harder radiation field. (52um was not observed.)

FIR line emitting regions: Example from Haro 11 (Cormier+13)



C_{HII}: compact, dense HII regions
 C_{PDR}: compact PDRs
 C_B: compact magnetic fields
 D_I: diffuse ionized media
 D_h: diffuse neutral media

2. Data

§2.1.6. summary of detections

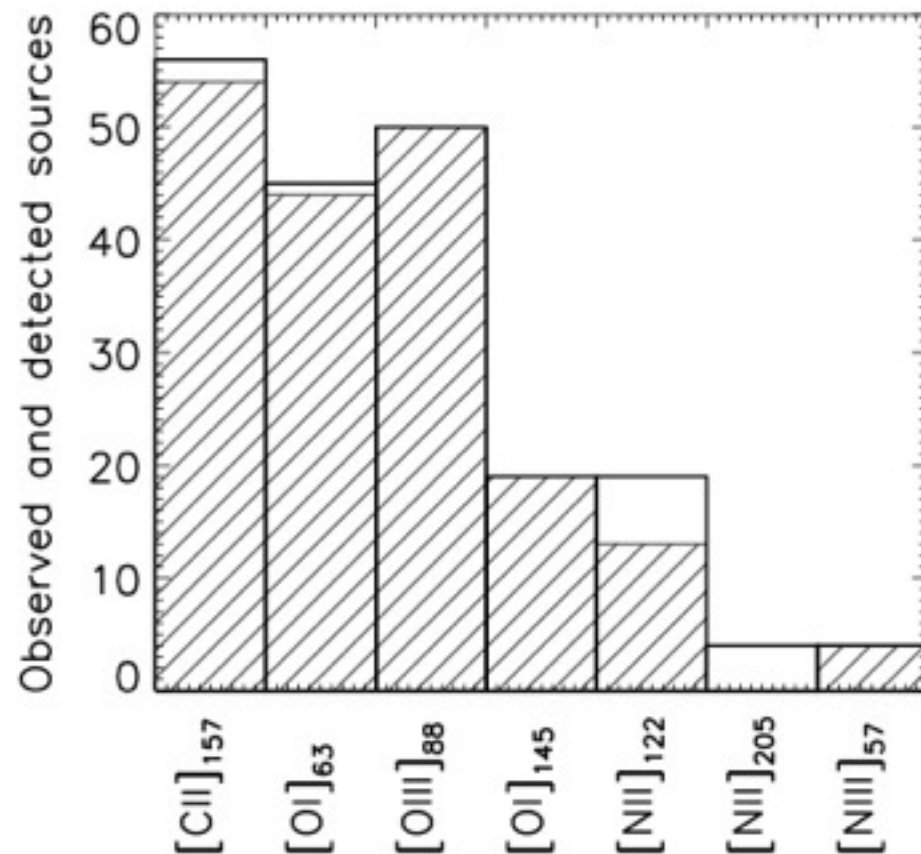
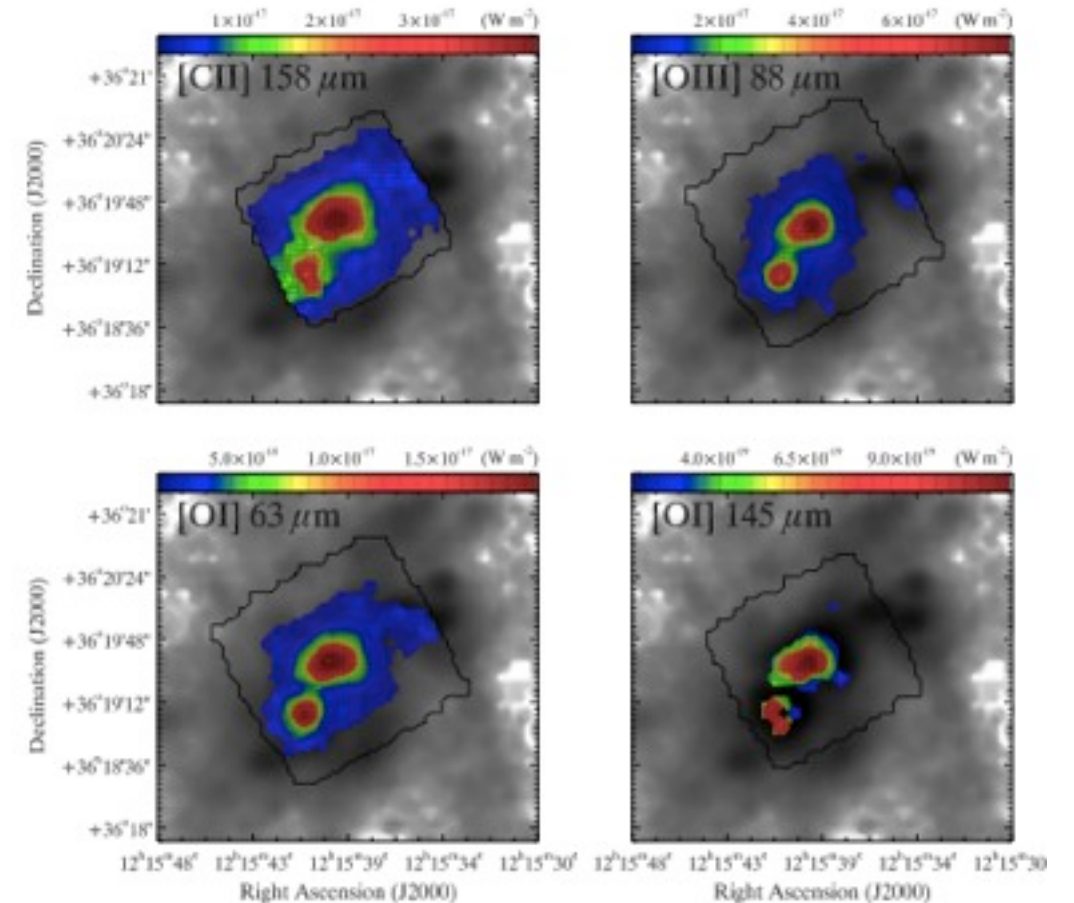


Fig. 1. For each PACS spectral line, the number of sources observed and detected (hashed) in the *Herschel* Dwarf Galaxy Survey.

[CII] peak: $4e-17 \text{ W m}^{-2}$ [OIII] peak: $8e-17 \text{ W m}^{-2}$



[OI] peak: $2e-17 \text{ W m}^{-2}$

NGC4214 from the DGS (Madden+2013)

- ❖ [CII]157, [OIII]88, and [OI]63 are the brightest.
- ❖ detected in >90%, on average >10x brighter than the other lines.

3. Observed ISM Properties

- ❖ Luminosity of FIR lines (§3.1)
- ❖ Effects of metallicity (§3.2)
- ❖ PACS line ratios (§3.3)
 - ❖ [OIII]/[NII]: different ionization potential (35.5 eV vs. 14.5 eV)
 - ❖ [NIII]/[NII]: different ionization potential (29.6 eV vs. 14.5 eV)
 - ❖ [OI]/[CII]: density and radiation strength
 - ❖ [OI]145/[OI]63: density and temperature
 - ❖ [OIII]/[OI]: filling factor of ionized gas
 - ❖ [NII]/[CII]: [CII] fraction from HII regions
- ❖ FIR line ([OIII], [CII], [OI]) to L_TIR ratios (§3.4)
 - ❖ to investigate variations in cooling by gas and dust, as a function of F60/F100 (\sim color temperature), L_{tir} (\sim galaxy size), and L_{tir}/L_B (\sim escape fraction).
- ❖ Summary of correlation analysis (§3.5)
 - ❖ Dwarfs have high [OIII]/[NII] (HII region), [CII]/[NII] ([CII] from PDRs), [OIII]/[OI] (HII region fill. factor), [CII]/L_{tir}, [OI]/L_{tir}, and [OIII]/L_{tir} ratios.
 - ❖ No clear correlation between emission and parameters (metallicity, F60/F100, L_{tir}, L_{tir}/L_B), indicating the properties are not controlled by a single param.
 - ❖ but by cloud physical conditions, mixing of ISM phases, geometry, dust properties, and photoelectric efficiency.

3. Observed ISM Properties

§3.1. Luminosity of FIR lines

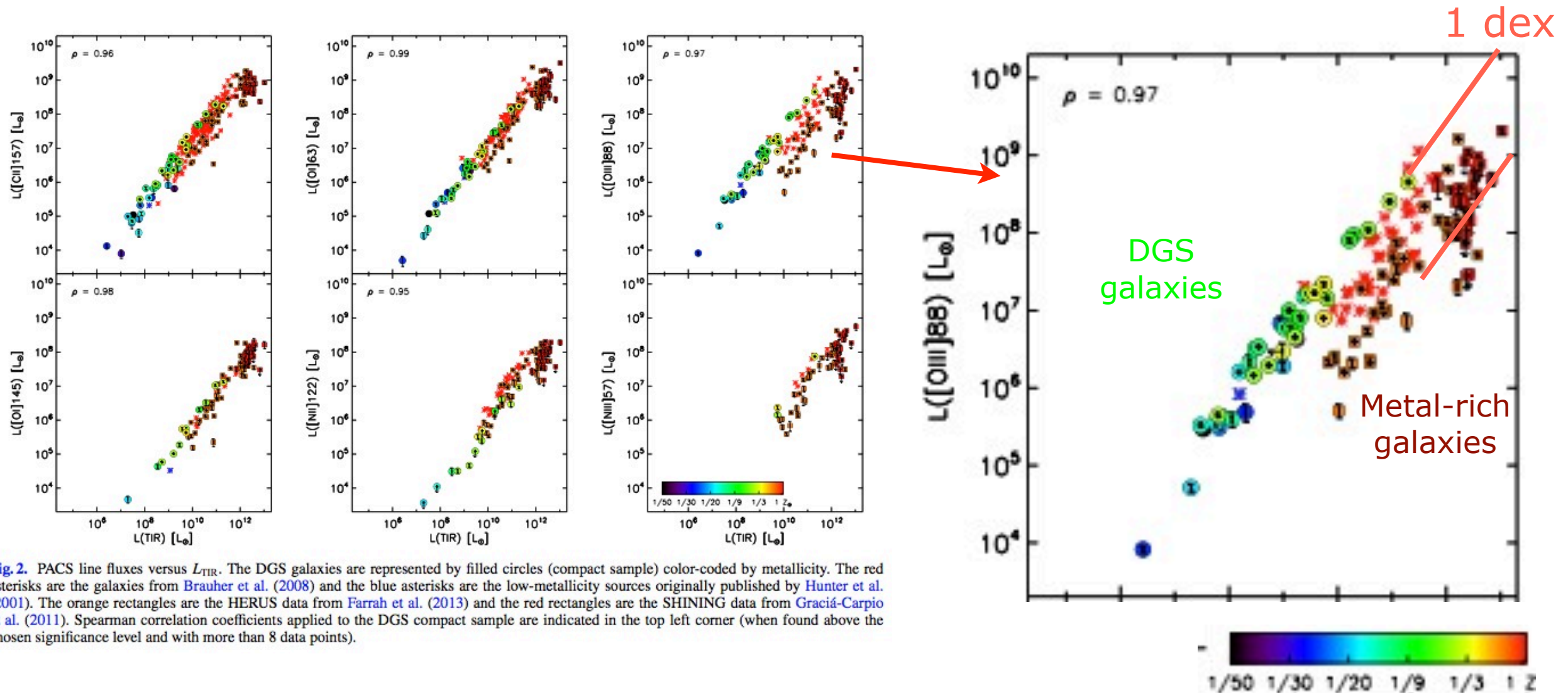


Fig. 2. PACS line fluxes versus L_{TIR} . The DGS galaxies are represented by filled circles (compact sample) color-coded by metallicity. The red asterisks are the galaxies from Brauher et al. (2008) and the blue asterisks are the low-metallicity sources originally published by Hunter et al. (2001). The orange rectangles are the HERUS data from Farrah et al. (2013) and the red rectangles are the SHINING data from Graciá-Carpio et al. (2011). Spearman correlation coefficients applied to the DGS compact sample are indicated in the top left corner (when found above the chosen significance level and with more than 8 data points).

- ❖ [OIII]88 is the brightest in most cases. [CII] / [OI]63 are the second / third brightest. [OI] dominates the cooling in resolved PDRs.
- ❖ FIR lines are correlated with L_{tir} (\sim size). Dispersion is smaller than ULIRGs (aka. line deficits).
- ❖ What is striking is the 1-dex offset between dwarfs and ULIRGs regarding [OIII].

3. Observed ISM Properties

§3.2. Effects of metallicity

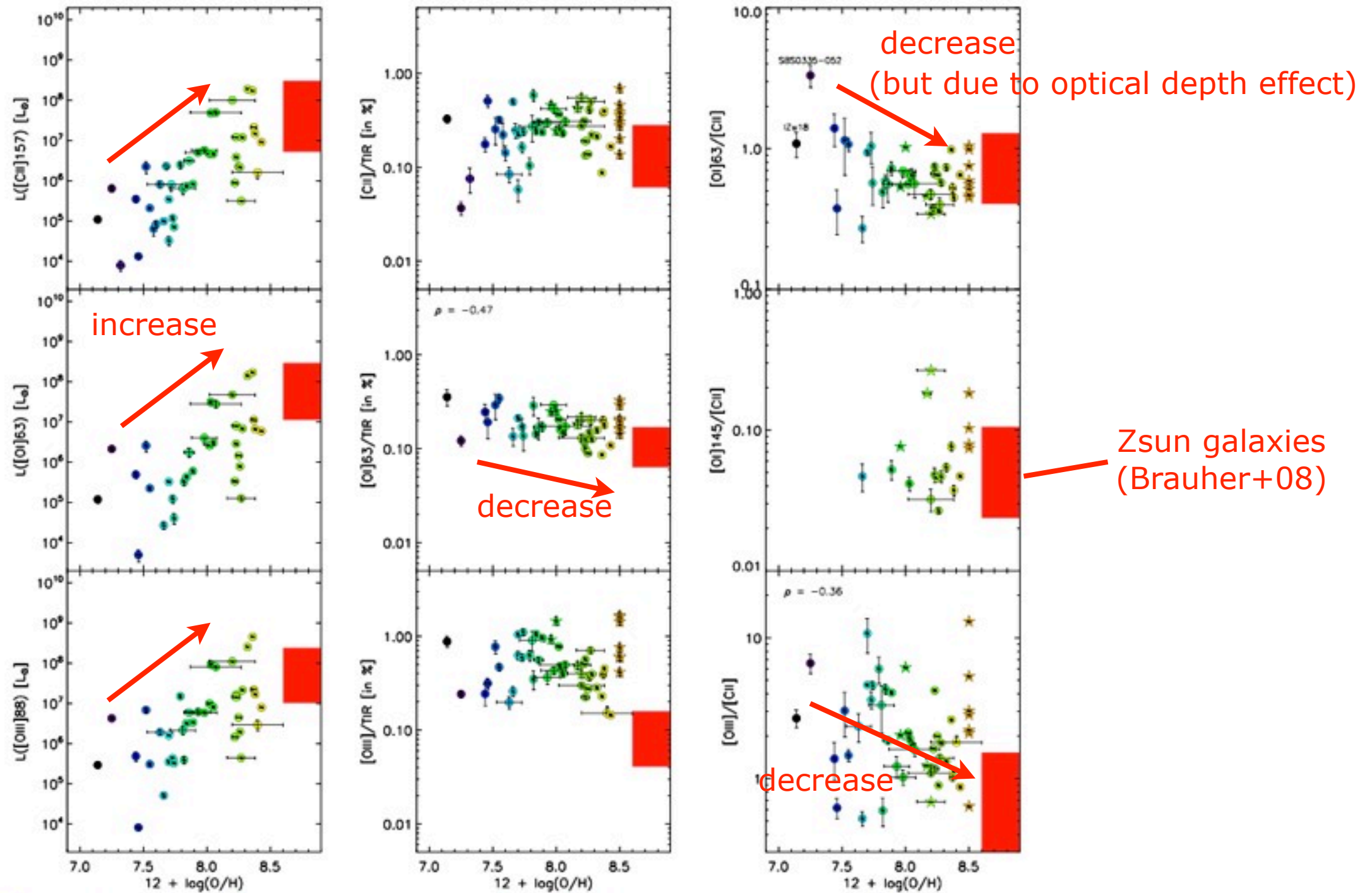


Fig. 3. PACS line fluxes, ratios, and line-to- L_{TIR} ratios as a function of metallicity. The DGS galaxies are represented by filled circles (compact sample) and stars (extended sample), color-coded by metallicity. Spearman correlation coefficients applied to the DGS compact sample are indicated in the top left corner (when found above the chosen significance level and with more than 8 data points). The large red rectangles show the range of values covered by the Brauher et al. (2008) sample, at metallicity around solar.

3. Observed ISM Properties

§3.3. PACS line ratios

In dwarf galaxies, ...

	Full DGS sample	Compact sample ^a	B08 sample
<i>PACS line ratio</i>			
[O I] ₆₃ /[C II] ₁₅₇	0.59 ^{3.31} _{0.27} (0.15 dex)	0.65 (0.20 dex)	0.72 (0.25 dex)
[O III] ₈₈ /[C II] ₁₅₇	2.00 ^{13.0} _{0.52} (0.34 dex)	1.79 (0.34 dex)	0.54 (0.45 dex)
[O I] ₁₄₅ /[O I] ₆₃	0.074 ^{0.17} _{0.041} (0.06 dex)	0.074 (0.05 dex)	0.063 (0.25 dex)
[O III] ₈₈ /[O I] ₆₃	2.96 ^{11.8} _{0.99} (0.24 dex)	2.66 (0.22 dex)	0.74 (0.25 dex)
[O III] ₈₈ /[N II] ₁₂₂	86.3 ⁴⁴² _{26.7} (0.23 dex) 30x	61.5 (0.22 dex)	3.27 (0.37 dex)
[N III] ₅₇ /[N II] ₁₂₂	8.06 ^{9.86} _{5.75} (0.13 dex)	8.06 (—)	1.91 (0.57 dex)
[N II] ₁₂₂ /[C II] ₁₅₇	0.025 ^{0.054} _{0.015} (0.23 dex)	0.022 (0.27 dex)	0.12 (0.21 dex)
[N III] ₅₇ /[O III] ₈₈	0.17 ^{0.29} _{0.067} (0.52 dex)	0.17 (0.37 dex)	1.08 (0.44 dex)
[N II] ₂₀₅ /[N II] ₁₂₂	<1	—	—
<i>Line-to-L_{TIR} ratio [in %]</i>			
[C II] ₁₅₇ /L _{TIR}	0.25 ^{0.69} _{0.04} (0.24 dex)	0.25 (0.22 dex)	0.13 (0.33 dex)
[O I] ₆₃ /L _{TIR}	0.17 ^{0.36} _{0.09} (0.14 dex)	0.17 (0.14 dex)	0.10 (0.21 dex)
[O III] ₈₈ /L _{TIR}	0.50 ^{1.66} _{0.15} (0.29 dex)	0.47 (0.26 dex)	0.080 (0.30 dex)
[O I] ₁₄₅ /L _{TIR}	0.011 ^{0.023} _{0.006} (0.19 dex)	0.010 (0.12 dex)	0.0065 (0.18 dex)
[N II] ₁₂₂ /L _{TIR}	0.0081 ^{0.0114} _{0.0028} (0.21 dex)	0.0060 (0.25 dex)	0.016 (0.19 dex)
[N III] ₅₇ /L _{TIR}	0.042 ^{0.111} _{0.026} (0.31 dex)	0.038 (0.07 dex)	0.043 (0.17 dex)
([C II] ₁₅₇ + [O I] ₆₃)/L _{TIR}	0.47 ^{1.04} _{0.16} (0.15 dex)	0.43 (0.17 dex)	0.26 (0.26 dex)
([C II] ₁₅₇ + [O I] ₆₃ + [O III] ₈₈)/L _{TIR}	1.03 ^{2.14} _{0.40} (0.18 dex)	0.97 (0.20 dex)	0.35 (0.26 dex)

-HII regions > PDRs

-filling factor of ion. gas

-HII regions > PDRs

-HII regions > diffuse ionized gas
-harder radiation field

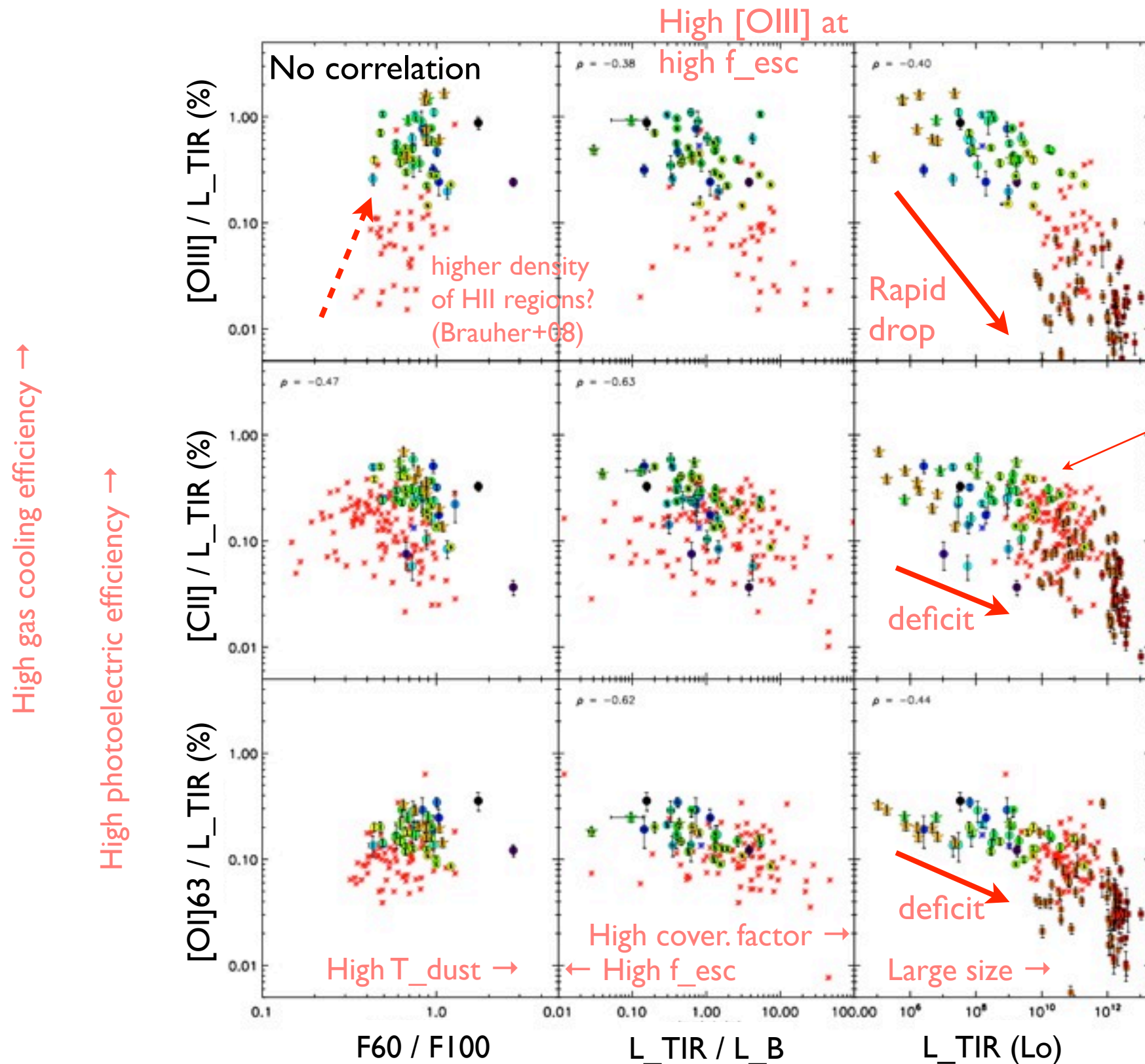
- high stellar T_{eff} (many OB stars)
- high filling factor of low-density, high-excitation gas

-negligible contribution from HII region to [CII] luminosity

FIR lines are important coolant

3. Observed ISM Properties

§3.4. FIR line-to- L_{TIR} ratios



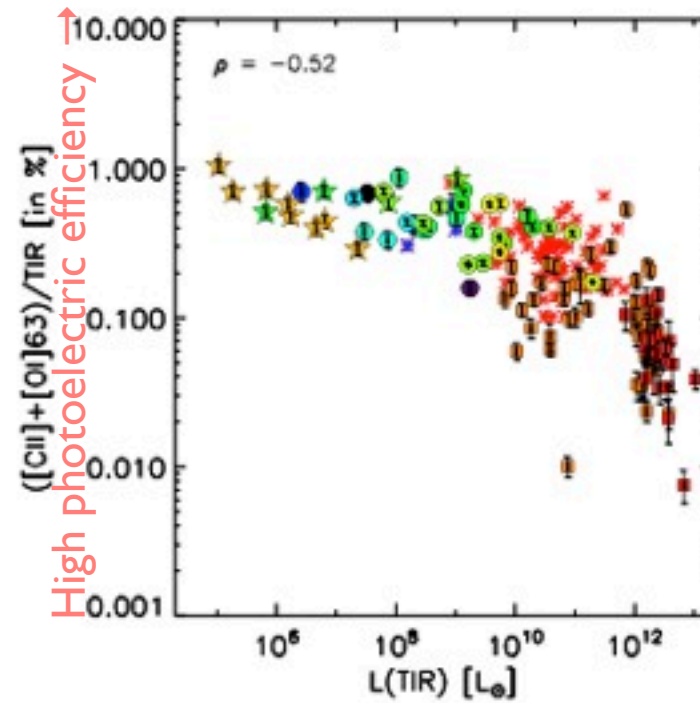
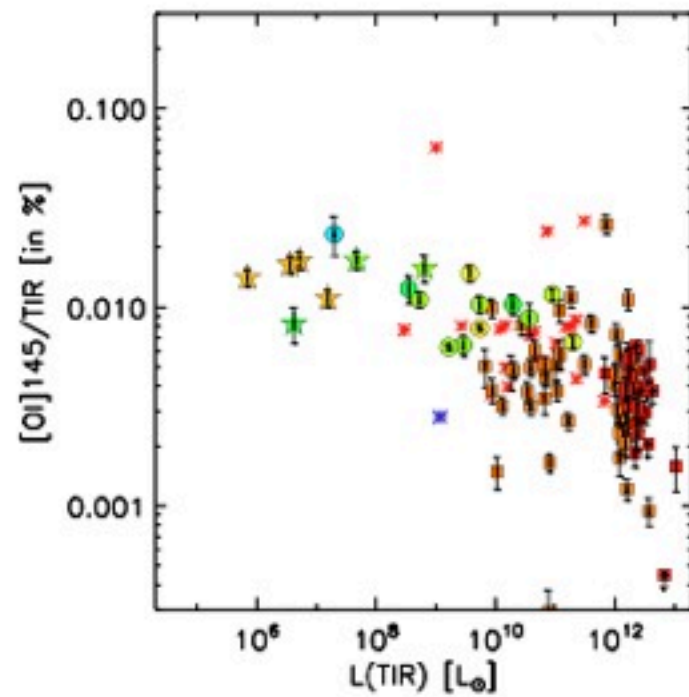
- High [OIII] at high f_{esc} suggests enhanced ISM proisity with lower L_{tir} and L_{tir}/L_B , which allows UV photons to excite O^{++} on larger scales.

- scatter may be due to different fractions of contributions from HII and PDR.

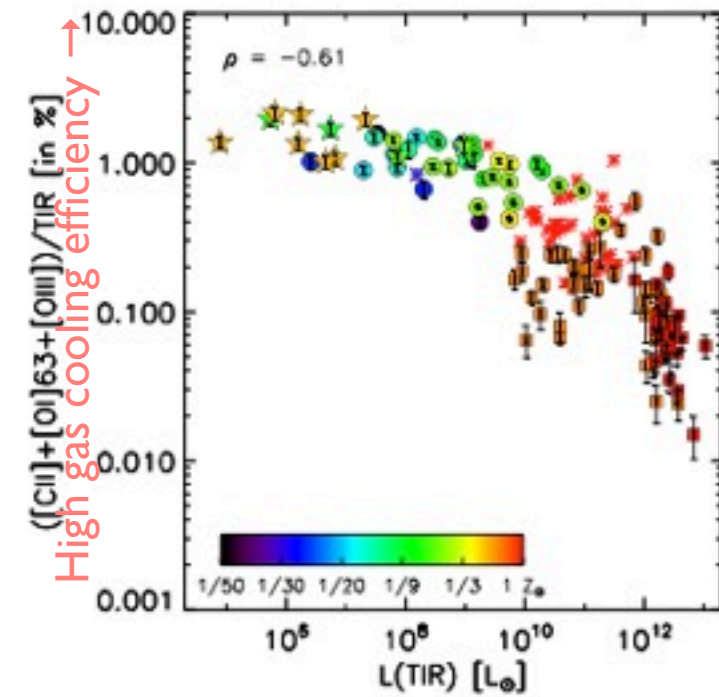
- High photoelectric efficiency in PDRs of dwarfs
 - High gas cooling efficiency in dwarfs

3. Observed ISM Properties

§3.4. FIR line-to- L_{TIR} ratios



- High photoelectric efficiency in PDRs of dwarfs



- High gas cooling efficiency in dwarfs

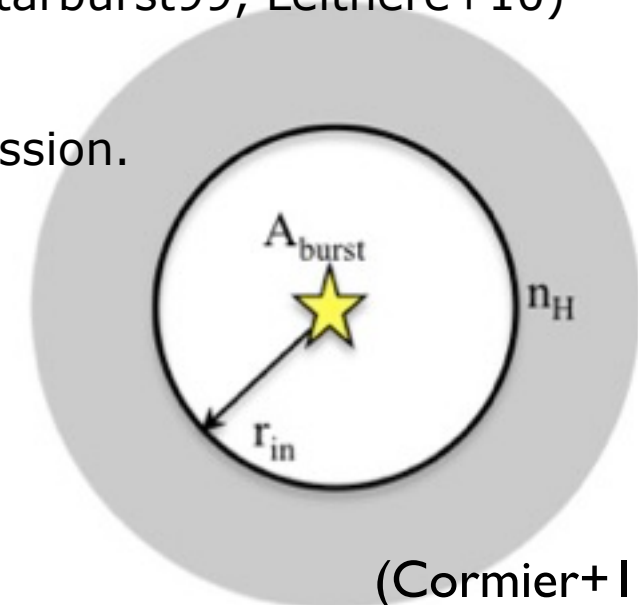
4. Trend analysis with radiative transfer models

- ❖ What are the parameters (see below) which reproduce the observed line ratios for dwarf galaxies?
- ❖ Modeling with CLOUDY (Ferland+13)
 - ❖ Free parameters
 - ❖ Hydrogen density: n_H ($10^1 \rightarrow 10^5 \text{ cm}^{-3}$)
 - ❖ Inner radius: r_{in} (15 \rightarrow 3200 pc) # distance between SB and surface of the modeled ISM shell.
 - ❖ Converted into
 - ❖ Ionization parameter (\sim age of burst): $U = Q(H) / (4 \pi r_{in}^2 n_H c)$
 - ❖ FUV radiation strength: G_0
- ❖ Configurations
 - ❖ Two metallicities: $2 Z_{ISM}$ and $1/4 Z_{ISM}$
 - ❖ Young starburst (10 Myr continuous) with $1e9 L_{\odot}$ (starburst99, Leithere+10)
 - ❖ DGR, PAH/H, PAH/dust, turbulent velo.
 - ❖ Stop calculations at $A_V = 10$ to fully model PDR emission.

Reference ISM abundances (Z_{ISM}):
 $O/H = 3.2 \times 10^{-4}$, $C/H = 1.4 \times 10^{-4}$, $N/H = 8 \times 10^{-5}$
 $Ne/H = 1.2 \times 10^{-4}$, $S/H = 3.2 \times 10^{-5}$

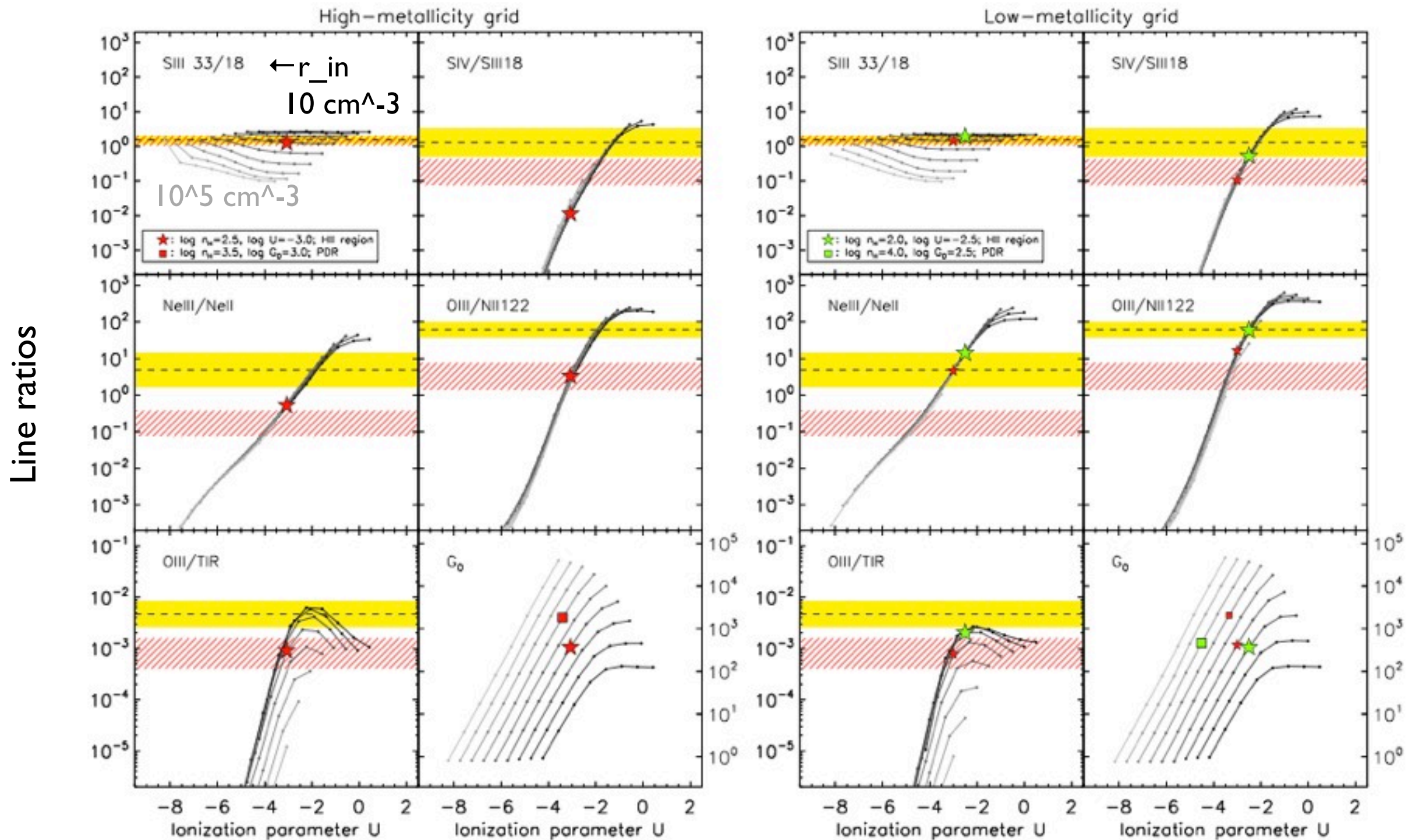
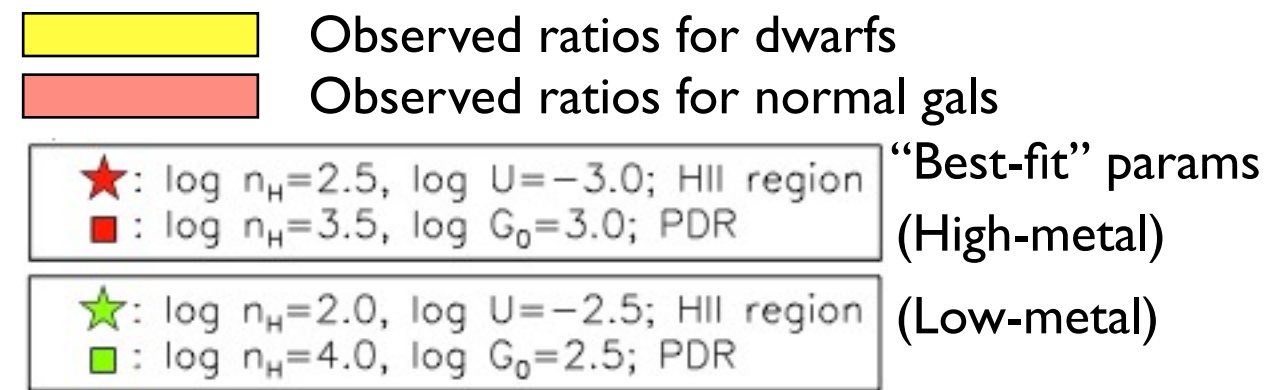
❖ Results

H II region fiducial model	Metal-rich	DGS sample
density [cm^{-3}]	$10^{2.5}$	$10^{2.0}$
$\log U$	-3.0	-2.5
$R_{S,eff}$ [pc]	16	46
PDR fiducial model		
density [cm^{-3}]	$10^{3.5}$	$10^{4.0}$
$\log G_0$	3.3	2.7



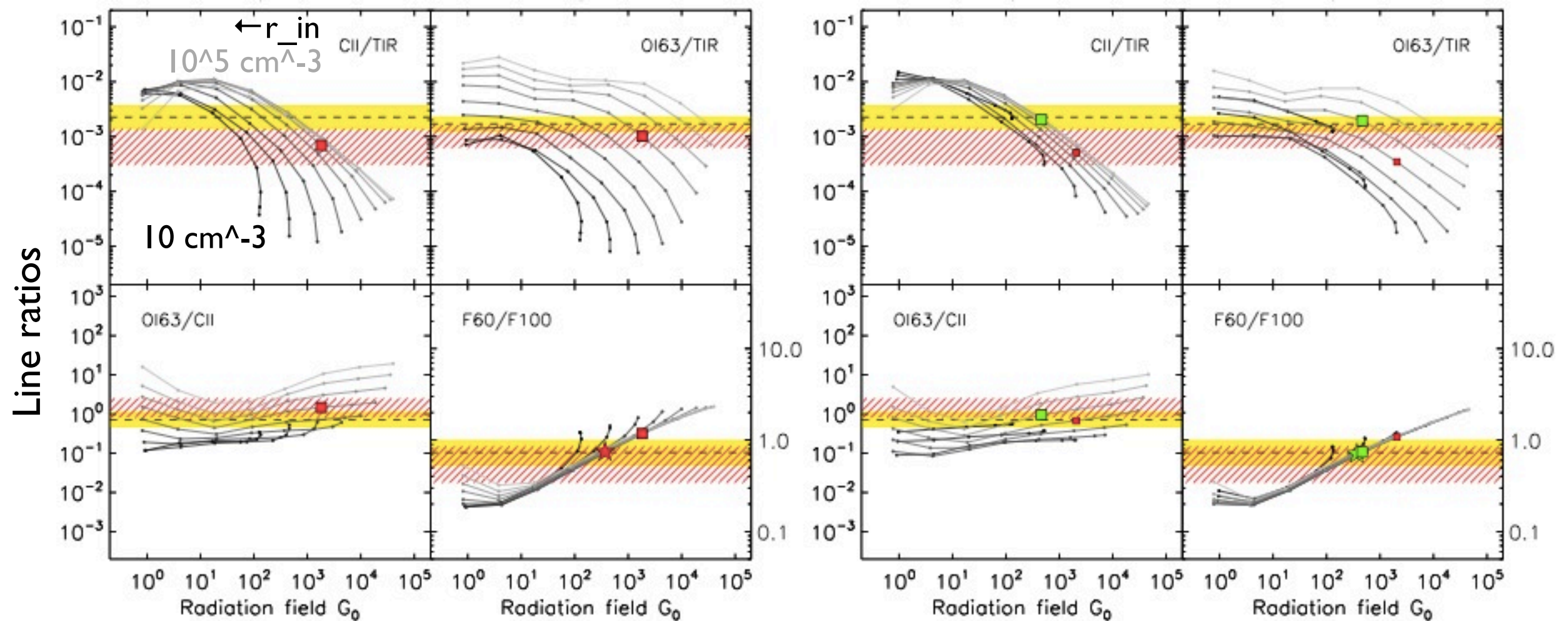
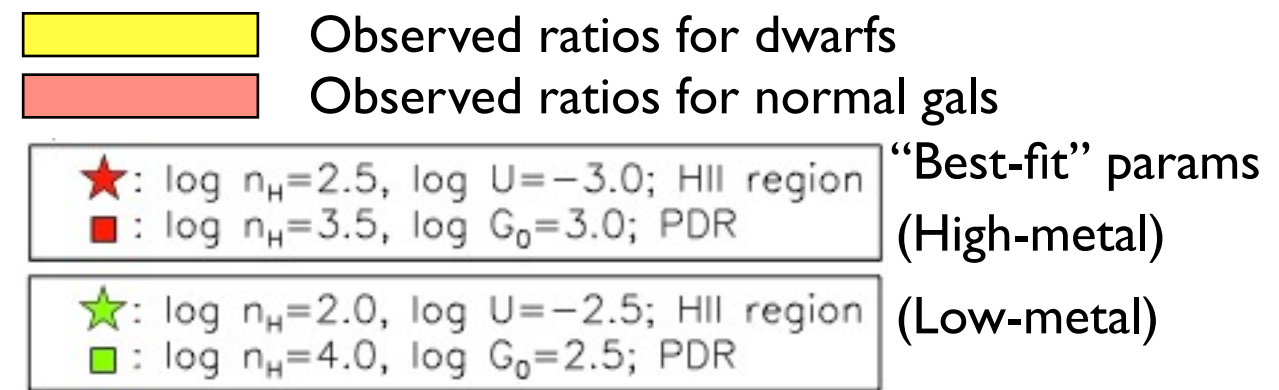
(Cormier+13)

Nebular lines



What are the parameters which reproduce the observed ratios? → ★ (for hi-metal), ★ (for low-metal)

PDR lines



What are the parameters which reproduce the observed ratios?

→ ■ (for hi-metal), ■ (for low-metal)

5. Discussion

- ❖ Effective Stromgren radius $R_{S,eff}$
 - ❖ 3x larger for dwarfs ($R_{S,eff} = 46$ pc) than metal-rich galaxies ($R_{S,eff} = 16$ pc), suggesting deeper penetration of ionizing photons in dwarf galaxies.
- ❖ Enhanced [OIII]/L_{tir} ratio in dwarf model (low-metallicity grid)
 - ❖ should be accounted for by reducing the mean A_v .
 - ❖ Emission from the PDR must be reduced relative to that of the HII region, by a factor of ~ 3 in DGS sample. (i.e. lower covering factor)
 - ❖ Consistent with the trend of decreasing [OIII]/L_{tir} with increasing L_{tir}/L_B. (§3.4)
 - ❖ Higher escape fraction in dwarfs is also observed in their SEDs (e.g., Galliano +2008)
- ❖ Change in the ISM structure and PDR distribution of low-metallicity galaxies
 - ❖ The filling factor of ionized gas relative to PDRs is higher than metal-rich galaxies.
 - ❖ The extent of HII region is bigger and UV photons travel larger distance.
 - ❖ The results suggest a more porous structure than that of metal-rich galaxies, which allows FUV photons to escape from a dwarf galaxy.

6. Conclusions (Abstract)

低金属環境下での FIR fine structure line の“出方”が違うが、なぜかはよくわかっていない。

目的は、低金属 ISM をもつ dwarf での FIR line の出方をしらべ、説明すること。

- PACS による 48 dwarfs の FIR line 観測
- line/TIR ratio と各種物理量の相関関係
- Cloudy 輻射輸送モデル

Context. The far-infrared (FIR) lines are important tracers of the cooling and physical conditions of the interstellar medium (ISM) and are rapidly becoming workhorse diagnostics for galaxies throughout the universe. There are clear indications of a different behavior of these lines at low metallicity that needs to be explored.

Aims. Our goal is to explain the main differences and trends observed in the FIR line emission of dwarf galaxies compared to more metal-rich galaxies, and how this translates in ISM properties.

Methods. We present *Herschel*/PACS spectroscopic observations of the [C II] 157 μm , [O I] 63 and 145 μm , [O III] 88 μm , [N II] 122 and 205 μm , and [N III] 57 μm fine-structure cooling lines in a sample of 48 low-metallicity star-forming galaxies of the guaranteed time key program Dwarf Galaxy Survey. We correlate PACS line ratios and line-to- L_{TIR} ratios with L_{TIR} , $L_{\text{TIR}}/L_{\text{B}}$, metallicity, and FIR color, and interpret the observed trends in terms of ISM conditions and phase filling factors with Cloudy radiative transfer models.

Results. We find that the FIR lines together account for up to 3 percent of L_{TIR} and that star-forming regions dominate the overall emission in dwarf galaxies. Compared to metal-rich galaxies, the ratios of [O III]₈₈/[N II]₁₂₂ and [N III]₅₇/[N II]₁₂₂ are high, indicative of hard radiation fields. In the photodissociation region (PDR), the [C II]₁₅₇/[O I]₆₃ ratio is slightly higher than in metal-rich galaxies, with a small increase with metallicity, and the [O I]₁₄₅/[O I]₆₃ ratio is generally lower than 0.1, demonstrating that optical depth effects should be small on the scales probed. The [O III]₈₈/[O I]₆₃ ratio can be used as an indicator of the ionized gas/PDR filling factor, and is found to be ~ 4 times higher in the dwarfs than in metal-rich galaxies. The high [C II]/ L_{TIR} , [O I]/ L_{TIR} , and [O III]/ L_{TIR} ratios, which decrease with increasing L_{TIR} and $L_{\text{TIR}}/L_{\text{B}}$, are interpreted as a combination of moderate far-UV fields and a low PDR covering factor. Harboring compact phases of a low filling factor and a large volume filling factor of diffuse gas, the ISM of low-metallicity dwarf galaxies has a more porous structure than that of metal-rich galaxies.

Key words. galaxies: dwarf – infrared: ISM – photon-dominated region (PDR) – techniques: spectroscopic – radiative transfer – HII regions

- 電離ガス/PDRの filling factor は、通常より高い
- line-to-TIR ratio が高いのは、moderate FUV 輻射場と low PDR filling factor のせい。すかすかな構造

- Dwarf では FIR line coolant の寄与が通常(Z-rich galaxies)より大きく (TIR の 3% まで)
- 星形成領域が全 luminosity を dominate
- 輻射場は硬い